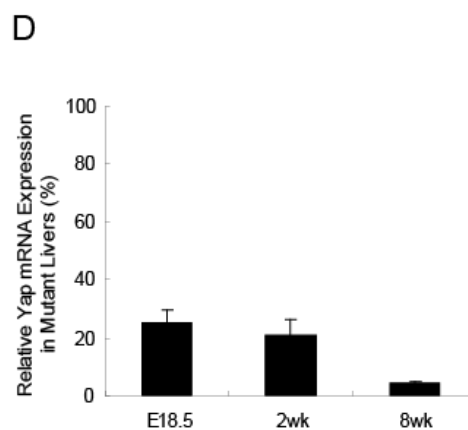
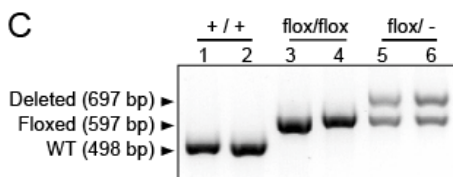
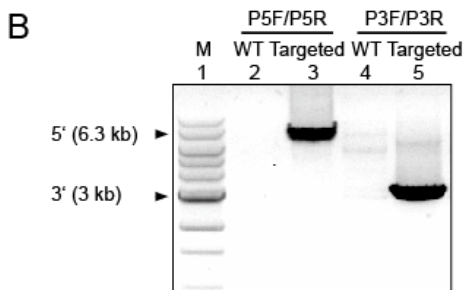
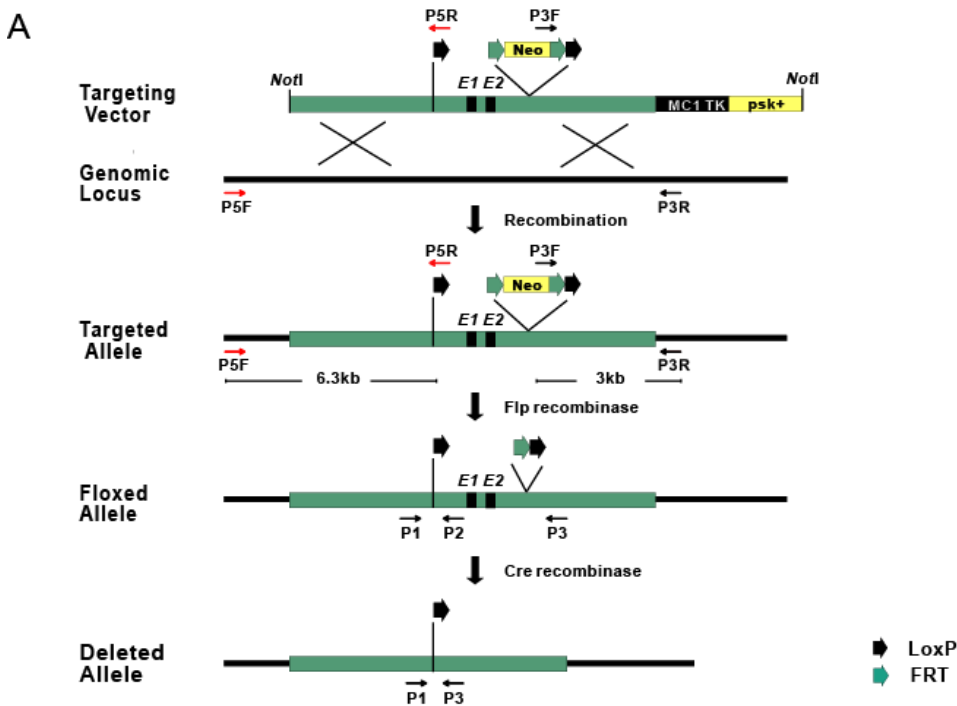


Supplemental Information

The Merlin/NF2 Tumor Suppressor Functions through the YAP Oncoprotein to Regulate Tissue Homeostasis in Mammals

Nailing Zhang, Haibo Bai, Karen K. David, Jixin Dong, Yonggang Zheng, Jing Cai, Marco Giovannini, Pentao Liu, Robert A. Anders, and Duoqia Pan

Figure S1. Generation of *Yap* conditional knockout mice, related to Figure 1



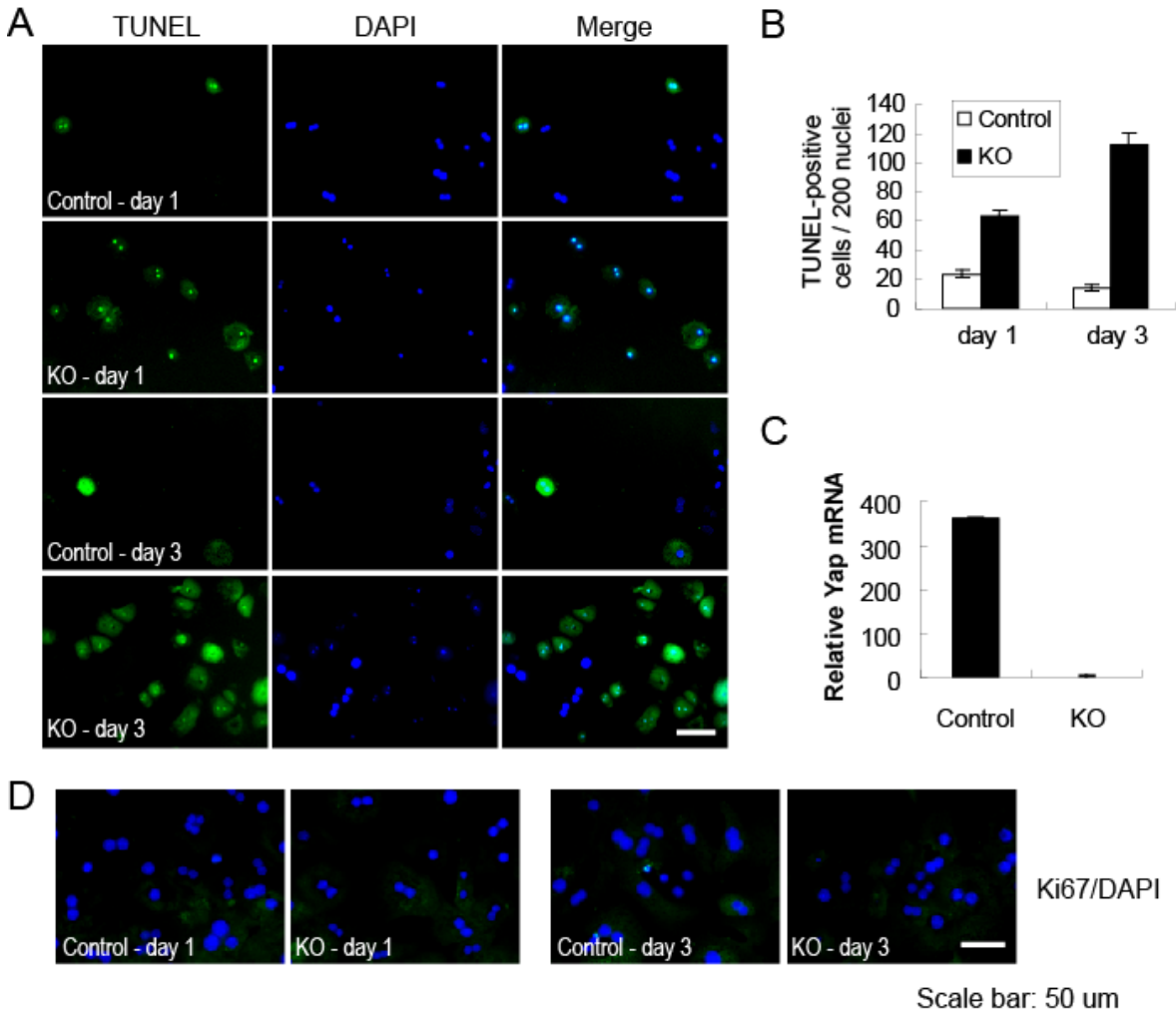
(A) Targeting strategy. Exons 1 and 2 of the *Yap* gene are indicated by black blocks. LoxP and FRT sites are indicated by black and green arrows, respectively. Also shown are the neomycin resistance gene (Neo) and PCR primers used for genotyping.

(B) Long-template PCR genotyping of mice with the targeted allele. Primers P5F and P5R amplify a PCR product of ~ 6.3 kb from the 5' region; primers P3F and P3R amplify a PCR product of ~ 3 kb from the 3' region. See (A) for schematic position of the PCR primers.

(C) PCR genotyping of mice with wildtype allele, floxed allele, or deleted allele using a mixture of primers P1, P2, and P3. See (A) for schematic position of the PCR primers.

(D) Relative *Yap* mRNA levels in Alb-Cre; *Yap*^{flox/flox} mouse livers compared to wildtype littermates at E18.5, 2 weeks, and 8 weeks of age, measured by qRT-PCR. Values are means ± SEM (n=3).

Figure S2. Increased apoptosis of *Yap*-deficient hepatocytes *in vitro*, related to Figure 2



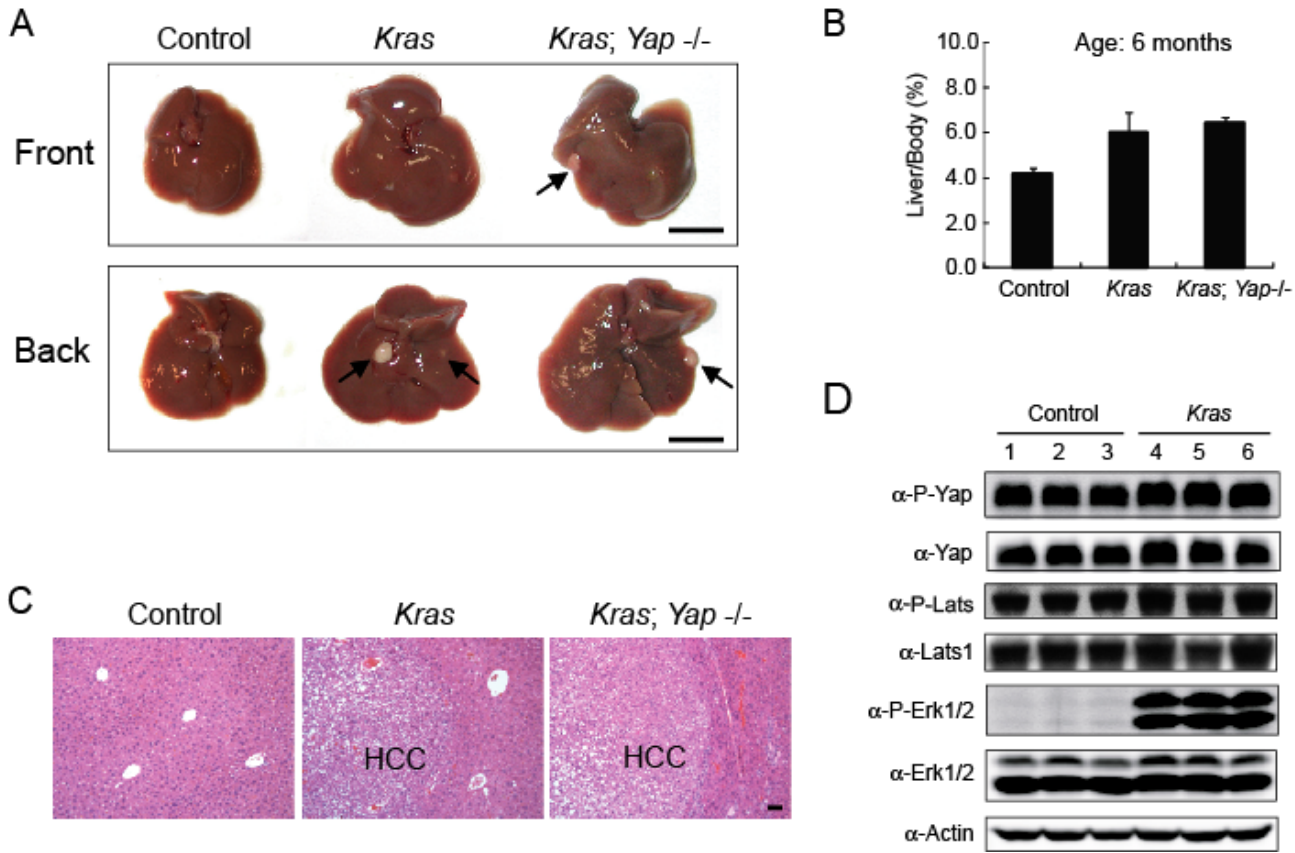
(A-B) Primary hepatocytes were isolated from control and *Yap*-deficient livers and plated as triplicate *in vitro*. At day 1 or day 3 after plating, the primary hepatocytes were analyzed for cell death using TUNEL staining (green). Note the dramatic increase of TUNEL-positive cells in *Yap*-deficient hepatocytes, which was quantified in (B). Values are means ± SEM (n=3).

(C) Quantitative real-time PCR analysis of *Yap* mRNA levels from primary hepatocytes isolated from control and *Yap*-deficient livers. *Yap* mRNA levels were reduced by 361-fold (*Yap* mRNA levels in *Yap*-KO livers were set as 1). Values are means ± SEM (n=3).

(D) Similar to (A) except that primary hepatocytes *in vitro* were analyzed for cell proliferation by Ki67 staining (green). Neither type of hepatocytes proliferates under our culture conditions.

Scale bars = 100 μ m.

Figure S3. Loss of *Yap* does not suppress RAS-induced HCC formation, related to Figure 3



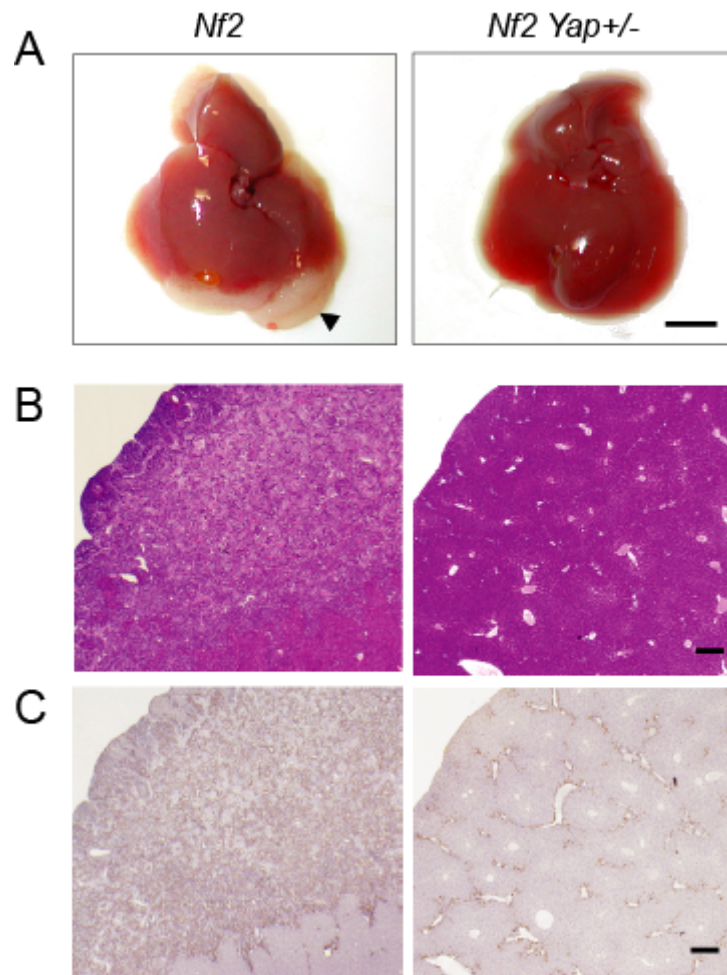
(A) Gross images of livers from wildtype control (left), *Alb-Cre; Lox-Stop-Lox-Kras^{G12D}* (middle) and *Alb-Cre; Lox-Stop-Lox-Kras^{G12D}; Yap^{lox/lox}* (right) at 6-month of age. Both front and back views are shown. Note the hepatomegaly and HCC nodules (arrows) in *Kras^{G12D}* and *Kras^{G12D} Yap* livers. Scale bar = 1 cm.

(B) Quantification of liver/body weight ratio in the respective genotype. Values are means \pm SEM (n=3).

(C) H&E staining showing the prevalence of HCC in 6-month-old *Kras^{G12D}* and *Kras^{G12D} Yap* livers. Scale bar = 50 μ m.

(D) Oncogenic *Kras* leads to Erk 1/2 activation but does not reduce YAP or Lats1/2 phosphorylation. Western blot analysis of liver lysates from 2-month-old control and *Alb-Cre; Lox-Stop-Lox-Kras^{G12D}* mice. Liver lysates from 3 mice of each genotype were probed with antibodies against P-YAP, YAP, P-Lats, Lats1, P-Erk1/2, Erk1/2 and Actin. Note the robust activation of Erk1/2 phosphorylation in *Kras^{G12D}* livers.

Figure S4. Suppression of *Nf2* mutant liver phenotypes by *Yap* Heterozygosity, related to Figure 4



(A) Gross liver images from two 1-month-old littermates. Note the thick hamartoma structure (arrowhead) at the edge of the *Nf2* mutant liver (left) and its absence in the *Nf2 Yap+/-* liver (right). Scale bars = 0.5 cm. (B-C) H&E (B) and CK staining (C) showing the prevalence of bile duct hamartoma in 1-month-old *Nf2* mutant livers (left) and the absence of hamartoma in *Nf2 Yap+/-* livers (right). Scale bar = 250 μ m.